

# The DØ Detector at the Fermilab Tevatron in Run 2

NEETI PARASHAR  
(for the DØ Collaboration)

111 Dana Research Center, Northeastern University  
360 Huntington Avenue, Boston, MA 02115, USA

## Abstract

The DØ (DZERO) Detector at Fermilab has been collecting data since March 1, 2001. The detector has undergone an extensive upgrade to participate in the Run 2 data taking. The design of the detector meets the requirements of the high luminosity environment provided by the accelerator. This paper describes the upgraded detector subsystems and gives an outline of the physics potentials associated with the upgrade.

## 1 Introduction

The Tevatron collider at the Fermi National Accelerator Laboratory in Illinois, USA, is the world's highest energy accelerator, colliding protons and antiprotons at a center of mass energy of almost 2 TeV. The DØ detector is designed to study collisions between these protons and anti-protons. DØ took its first data run in the period 1992-1996, called Run I, with an energy of 1.8 TeV, 6x6 proton and antiproton bunches (3.5  $\mu$ s between crossings) and luminosities of order  $10^{31}$  cm<sup>-2</sup>s<sup>-1</sup>. Between 1996 and 2001, major upgrades were undertaken both to the detector and to the accelerator complex. Notably, a new 150 GeV synchrotron, the Main Injector, was constructed to replace the old Main Ring as the injector to the Tevatron. With this new machine in operation, Run 2 began in 2001. The first phase, Run 2a, has seen the energy raised to 1.96 TeV, 36x36 proton and antiproton bunches (396 ns between crossings) and will have luminosities up to  $2 \times 10^{32}$  cm<sup>-2</sup>s<sup>-1</sup>. This will be followed by a short shutdown period to replace the present vertex detector. The second phase, Run 2b, will continue atleast until 2009 or until it becomes noncompetitive with the Large Hadron Collider (LHC) at CERN; in this period, the number of bunches will be increased to roughly 100x100 (132 ns between crossings) and the luminosity will rise to  $5 \times 10^{32}$  cm<sup>-2</sup>s<sup>-1</sup>. The total integrated luminosity foreseen for Run 2 is 15 fb<sup>-1</sup>. The performance of the upgraded detector can be found in [1]. The successes of Run I, including the discovery of the top quark, and the physics potential of high-luminosity running at the Tevatron have additionally motivated the present upgrade of the detector. We would now like to pursue a detailed top quark physics study, search for the Higgs boson and evidence of Supersymmetry, investigate b-physics, and study physics beyond the Standard Model (SM).

The upgrade consists of the addition of a cosmic ray scintillator shield and bunch tagging system, the replacement of the front-end electronics for the calorimeter and the muon system, the upgrade of the muon detection system, the replacement of the tracking system for both the central and forward regions, the addition of preshower detectors, and improvements to the trigger and data acquisition systems. Figure 1 shows an elevation view of the upgraded detector.

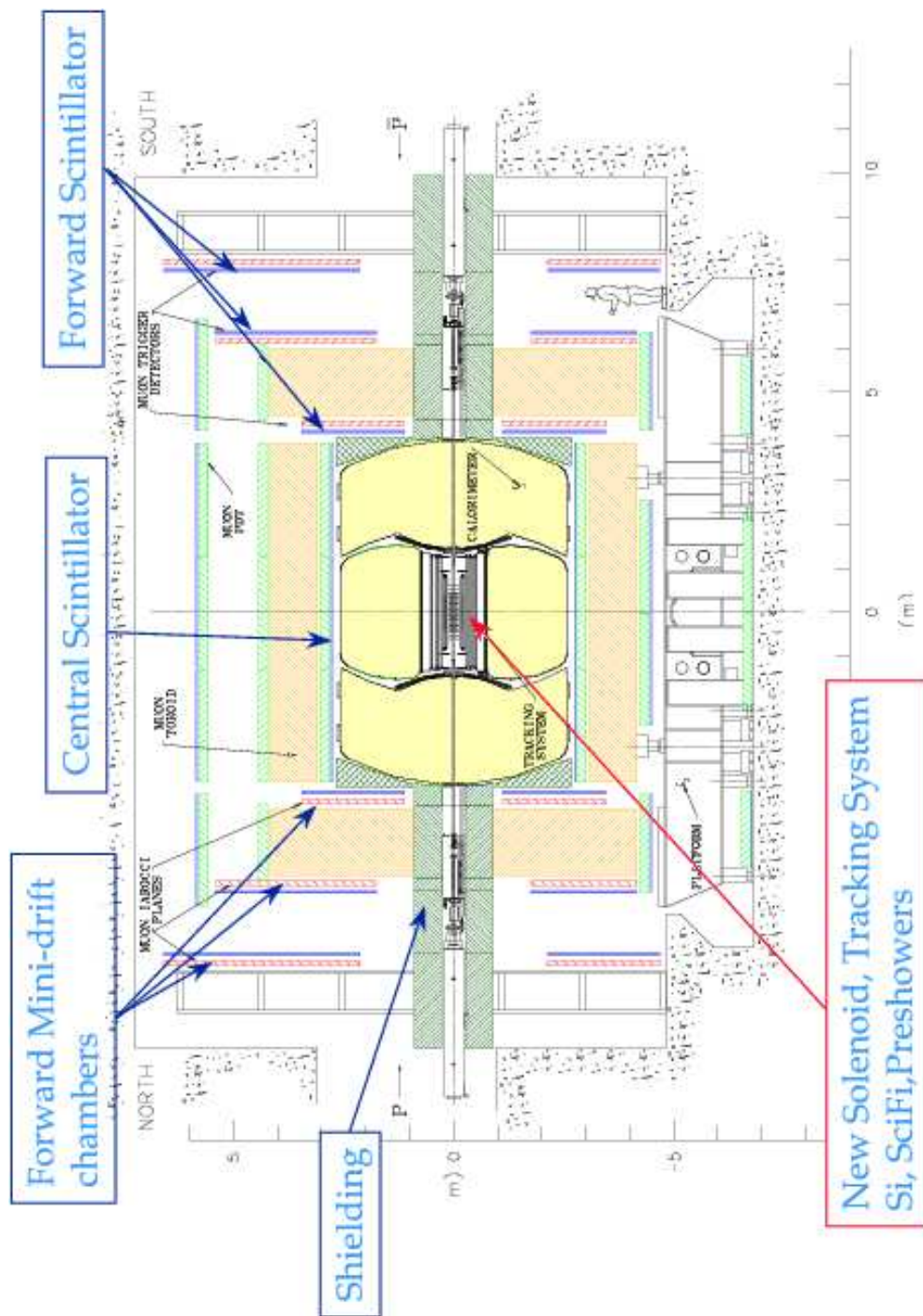


Figure 1: Elevation view of the upgraded DØ detector for Run 2.

## 2 Tracking

The tracking system (Fig. 2) consists of an inner silicon microstrip tracker (SMT), surrounded by a central scintillating fiber tracker (CFT). These systems are contained within the bore of a 2T superconducting solenoid, which is surrounded by a scintillator preshower detector.

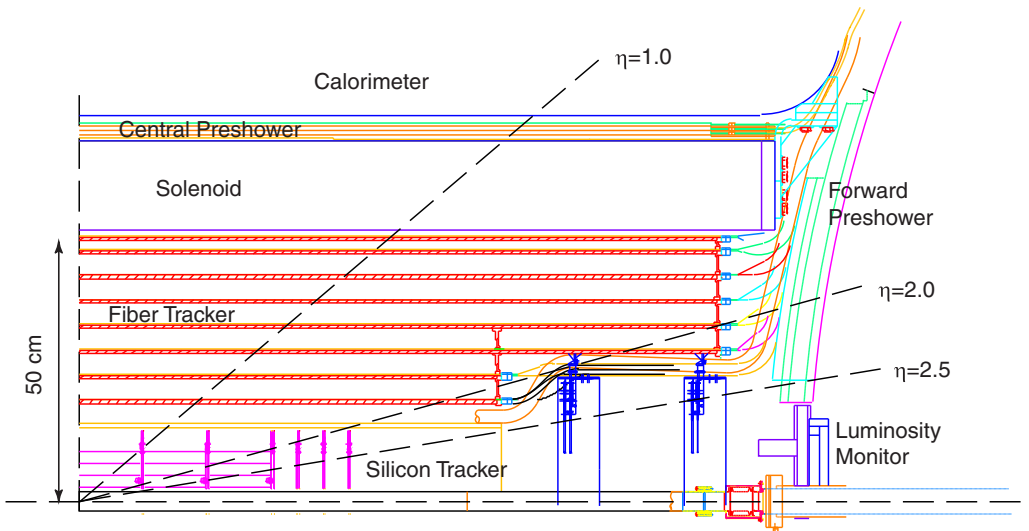


Figure 2:  $r - z$  view of the DØ tracking system.

The upgraded tracking system has been designed to meet several goals: momentum measurement by the introduction of a solenoid field; good electron identification and  $e/\pi$  rejection; tracking over a large range in pseudorapidity ( $|\eta| < 3$ ); secondary vertex measurement for identification of  $b$ -jets from Higgs and top decays and for  $b$ -physics; first level tracking trigger; fast detector response to enable operation with a bunch crossing time of 132 ns; and radiation hardness.

### 2.1 Silicon Microstrip Tracker (SMT)

The silicon tracking system is based on  $50 \mu\text{m}$  pitch silicon microstrip detectors, with a total of 793,000 channels, and provides a spatial resolution of approximately  $10 \mu\text{m}$  in  $r\phi$ . The high resolution is important to obtain good momentum measurement and vertex reconstruction. The detector consists of a system of barrels (Fig. 3) and interleaved disks designed to provide good coverage out to  $|\eta| \approx 3$  for all tracks emerging from the interaction region, which is distributed along the beam direction with  $\sigma_z \approx 25 \text{ cm}$ . The SVXIIe chip is used for readout [2]. Please refer to [3] for details.

A silicon track trigger preprocessor is being built that will allow use of SMT information at Level 2 trigger. This will add the capability for triggering on tracks displaced from the primary vertex, as well as sharpen the  $p_T$  threshold of the Level 2 track trigger and of the electron and jet triggers at Level 3 trigger.

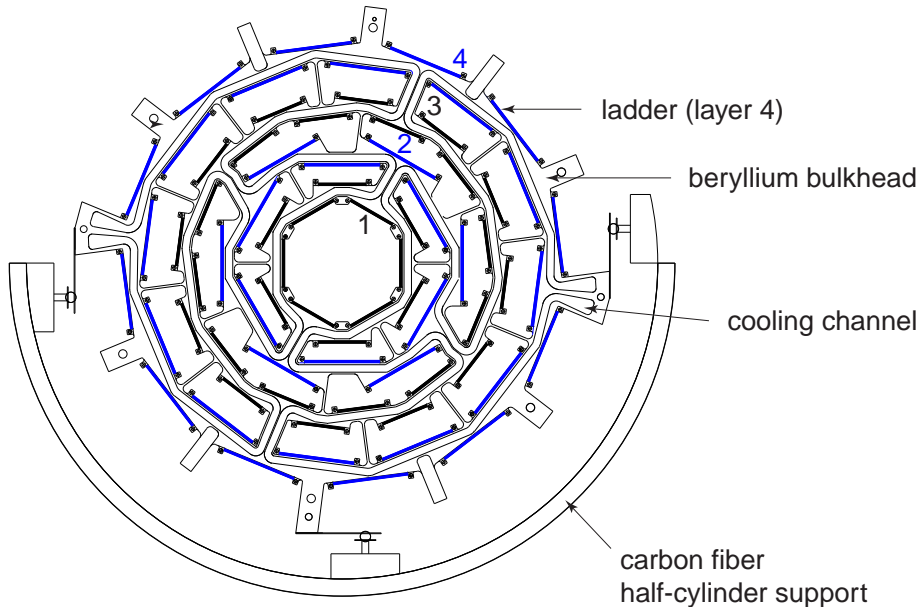


Figure 3: Cross sectional  $r\phi$  view of an SMT barrel.

## 2.2 Central Fiber Tracker (CFT)

The detector just outside the SMT is the 8-layered CFT, which is based on scintillating fiber ribbon doublets with visible light photon counter (VLPC) readout [4]. The CFT serves two main functions. First with the SMT, it enables track reconstruction and momentum measurement for  $|\eta| < 1.7$ , second it provides fast Level 1 triggering on charged track momentum. The details can be found in [3].

## 2.3 Superconducting Solenoid

The superconducting solenoid is 2.73 m in length and 1.42 m in diameter and provides a 2 T magnetic field, allowing charged particle momentum measurement. The solenoid is wound with two layers of multifilamentary Cu:NbTi wire strands stabilized with aluminum. Eighteen strands are used in each conductor. To ensure good field uniformity, the current density is larger at the ends of the coil. The thickness of the magnet system is approximately one radiation length.

## 3 Preshower detectors

The central and forward preshower detectors (CPS and FPS) provide fast energy and position measurements for the electron trigger and offline electron identification. The preradiator consists of 5.5 mm lead in the CPS and 11 mm of lead in the FPS (see Fig. 4).

The CPS detector consists of three concentric cylindrical layers of interleaved triangular scintillator strips. The three layers are arranged in an  $xuv$  geometry ( $x$  = axial,  $uv = \pm$  stereo angle of approximately  $23^\circ$ ). Wavelength shifting fibers are used to pipe the light out to a VLPC readout system.

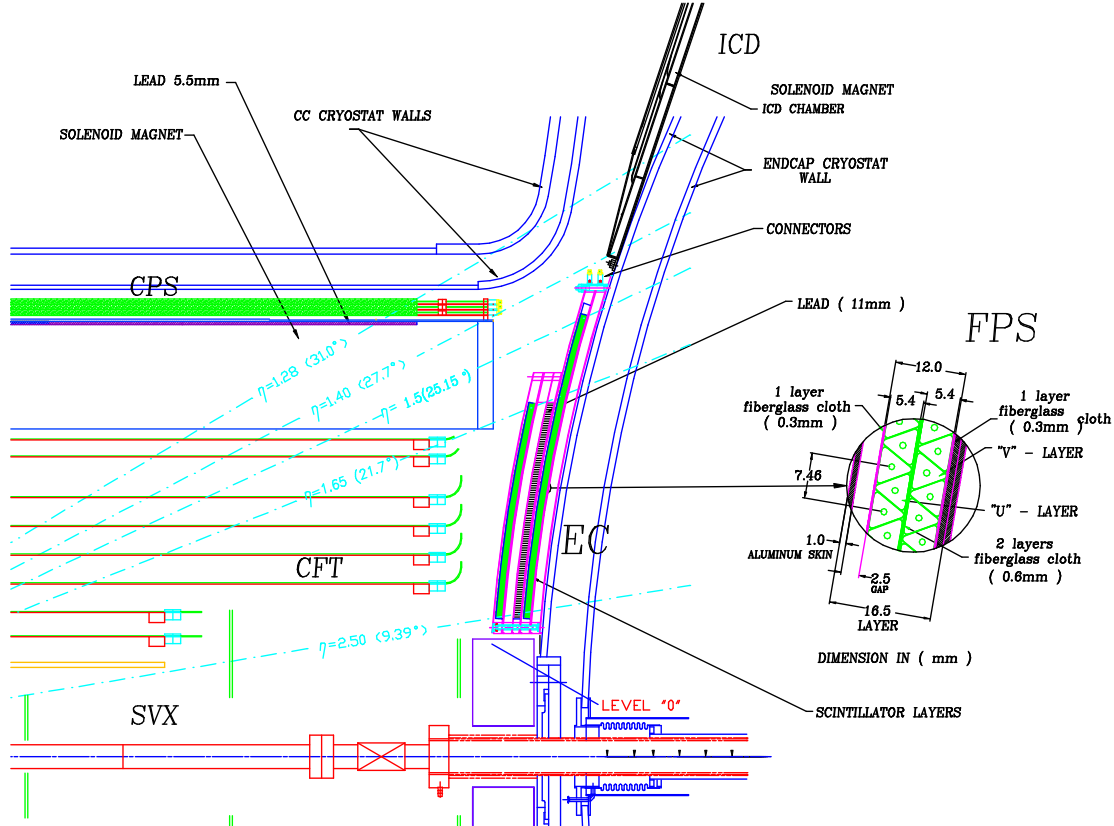


Figure 4: The central and forward preshower detectors, with a detail of the FPS construction.

The position resolution for 10 GeV electrons is estimated from Monte Carlo studies to be  $< 1.4$  mm. Cosmic ray tests have been performed to study the light yield and resolution [5]. Figure 5 shows some results. The light yield is shown in Fig. 5(a) together with the simulated yield for a cosmic ray muon passing through a “singlet” (i.e. a single layer of triangular strips) and a “doublet” (two layers of strips). The readout fiber in this setup was 11 m in length. Figure 5(b) shows the fitted track residuals. The measured doublet position resolution for cosmic ray muons is  $550 \mu m$ .

The forward preshower detector is constructed from two  $uv$  layers of triangular strips. A detail of the design is shown in Fig. 4.

## 4 Muon Detectors

The higher event rates in Run 2 have led us to add new muon trigger detectors which cover the full pseudorapidity range and the harsh radiation environment has prompted us to replace the forward proportional drift tubes (PDTs) with mini drift tubes (MDTs). In the central region, the existing proportional drift tubes were retained, but with the faster gas Ar-CH<sub>4</sub>-CF<sub>4</sub> (80%:10%:10%) resulting in a maximum drift time of 500 ns. The contribution to the hit position uncertainty due to diffusion is about  $375 \mu m$  (compared with  $300 \mu m$  for the slower Run I gas). However, the decreased number of proton-

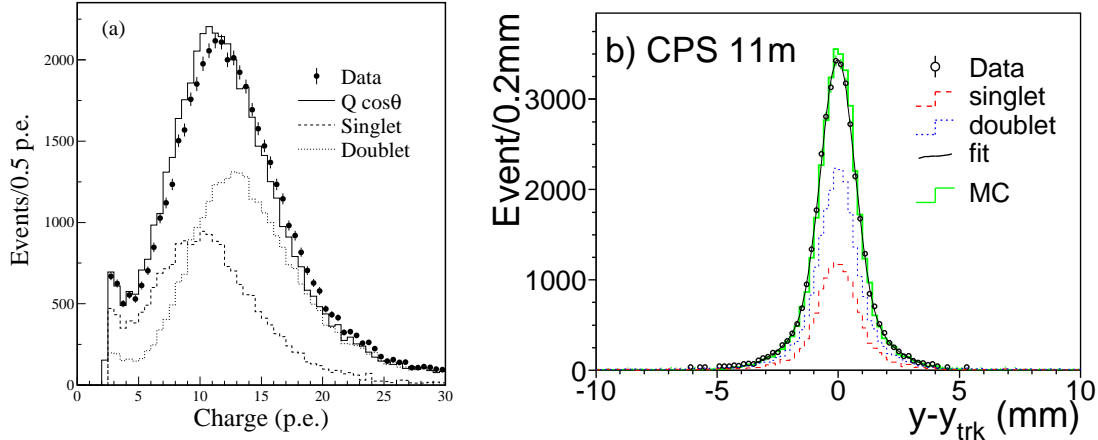


Figure 5: Preshower detector cosmic ray muon tests: (a) light yield (p.e. = photoelectrons); (b) fitted track residuals.

antiproton beam crossings within the drift time ( $\simeq 2$  for 396 ns operation and  $\simeq 4$  for 132 ns operations) results in reduced occupancy and improved triggering. The front end electronics has also been replaced to ensure deadtimeless operation. Further details can be found in [3].

The scintillation counters provide time information and are used to match the muon tracks in the fiber tracker. They have been organized into three layers to reduce hit combinatorics. The drift tubes provide enhanced muon momentum resolution and pattern recognition. The design of the muon system reduces backgrounds and trigger rates by providing additional shielding and DØ is able to trigger on inclusive single muons with  $p_T > 7$  GeV and dimuons with  $p_T > 2$  GeV.

## 5 Trigger and Data Acquisition

The DØ trigger and DAQ systems have been completely restructured to handle the shorter bunch spacing and new detector subsystems in Run 2. The level 1 and 2 triggers utilize information from the calorimeter, preshower detectors, central fiber tracker, and muon detectors. The level 1 trigger reduces the event rate from 7.5 MHz to 10 kHz and has a latency of 4  $\mu$ sec. The trigger information is refined at level 2 using calorimeter clustering and detailed matching of objects from different subdetectors. The level 2 trigger has an accept rate of 1 kHz and a latency of 100  $\mu$ sec. Level 3, consisting of an array of PC processors, partially reconstructs event data within 50 msec to reduce the rate to 50 Hz. Events are then written to tape.

## 6 Detector Performance

The Run I DØ detector has been very successful in measuring the properties of the Standard Model. New capabilities of the upgraded DØ detector include:

- Tag b-quark decays using displaced vertices in the silicon tracker
- Enhance muon identification and triggering, especially at low  $p_T$
- Enhance electron identification and triggering using the preshower and central tracking detectors
- Improve tau identification
- Determine the sign of charged particles and measure their momentum

The momentum resolution of the tracking system is shown in Fig. 6. At  $\eta = 0$  the resolution is approximately  $\delta p_T/p_T = 17\%$  for  $p_T = 100$  GeV. With this resolution the upgrade tracking will enable  $E/p$  matching for electron identification, will improve the muon momentum resolution and will provide charge sign determination for charged particles and help in calorimeter calibration.

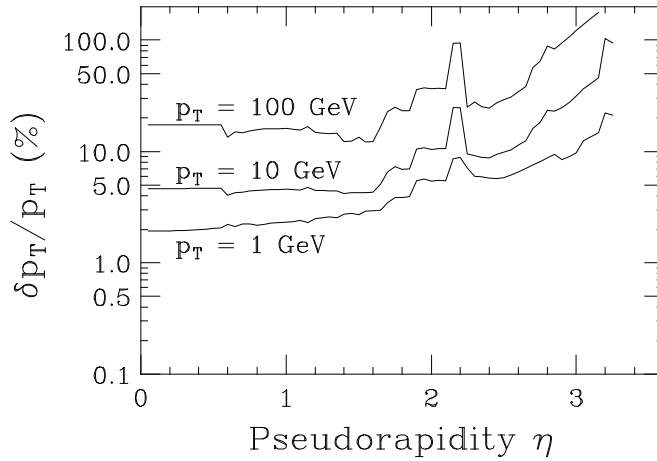


Figure 6: Transverse momentum resolution vs. pseudorapidity.

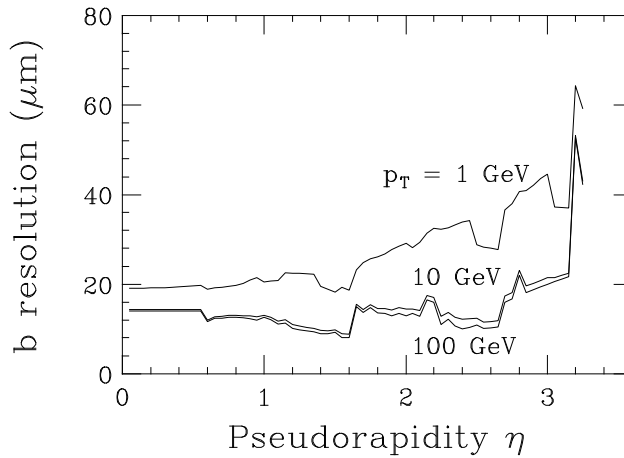


Figure 7: 2d impact parameter resolution in the  $r\phi$  plane vs. pseudorapidity.

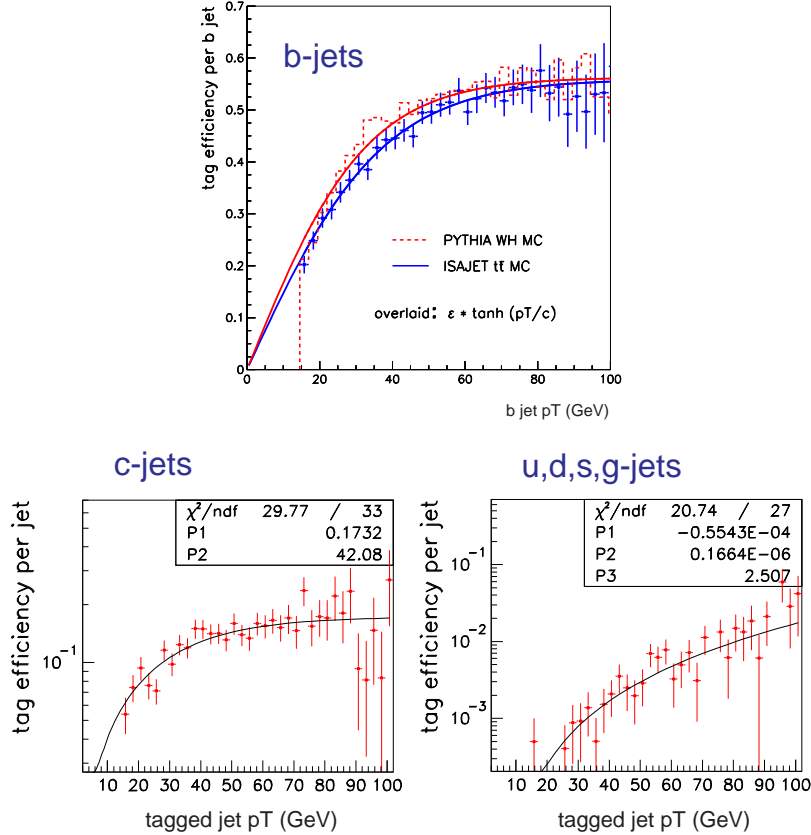


Figure 8: Efficiency for tagging  $b$ -jets,  $c$ -jets, and light-quark/gluon jets as a function of jet  $p_T$  from parameterized simulations of  $WH$  and  $t\bar{t}$  events.

The tracking system will also be used to tag displaced secondary vertices, especially important for the Higgs search, and for  $t\bar{t}$  physics and  $b$ -physics. Fig. 7 shows the resolution of the 2-dimensional  $r\phi$  impact parameter as a function of pseudorapidity. The resolution is less than 20  $\mu\text{m}$  for tracks with  $p_T < 1$  GeV over the approximate range  $|\eta| \leq 2$ , which is the region of interest for tagging  $b$ -jets from top decays. Based on a parameterized Monte Carlo simulations of PYTHIA  $p\bar{p} \rightarrow WH \rightarrow \ell\nu b\bar{b}$  events and ISAJET  $p\bar{p} \rightarrow t\bar{t} \rightarrow \ell\nu + \text{jets}$  events, we expect a  $b$ -tagging efficiency of  $\simeq 55\%$ , decreasing at low  $b$ -jet  $p_T$ , as shown in Fig. 8.

## 7 Run 2 Physics Prospects

We have seen that the design of the Run 2 DØ detector makes important additions to the physics capabilities, namely: energy/momentum matching for electron identification, improved muon momentum resolution, charged sign and momentum determination, calorimeter calibration and displaced vertex identification ( $b$ -tags).

One of the most important goals of Run 2 is the search for the Higgs boson. Assuming that the correct explanation of electroweak symmetry breaking is the Higgs mechanism, fits to electroweak data show that the Higgs mass is less than 170 GeV at the 95%

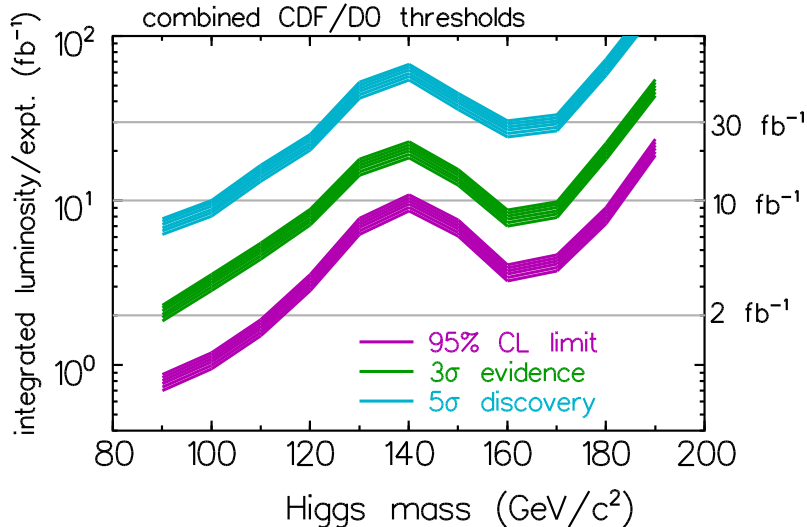


Figure 9: Integrated luminosity required as a function of Higgs mass for a 95% C.L. exclusion,  $3\sigma$  evidence and  $5\sigma$  discovery.

confidence level. Direct searches at LEP rule out a Higgs mass below 113 GeV, while recent indications from LEP suggest the possibility of a Higgs signal at  $m_H \simeq 115$  GeV [6]. This is precisely the Higgs mass range accessible at the Tevatron, provided sufficient integrated luminosity is achieved. The dominant Higgs production processes at the Tevatron are gluon fusion, ( $gg \rightarrow H$ ), and associated production with a  $W$  or a  $Z$  boson, ( $q\bar{q} \rightarrow W/ZH$ ). The gluon fusion process has a higher cross-section but is overwhelmed by the QCD background in the light mass region ( $m_H \leq 135$  GeV), where  $H \rightarrow b\bar{b}$  is the dominant decay channel. The associated production process, however, provides a handle to suppress the background even though the cross section is much smaller than the gluon fusion process.

Recently, there has been much attention paid to these Higgs searches, and detailed studies have been performed as part of the Tevatron Run 2 Workshop [7]. Fig. 9 shows the integrated luminosity delivered per experiment which would be required to exclude the SM Higgs at the level of 95%. The wide bands in the plot represent the calculated threshold plus uncertainties in the  $b$ -tagging efficiency, background rate, mass resolution, and other effects. As the plot shows, in order to cover the full possible spectrum of Higgs mass allowed at Tevatron energies, the total integrated luminosity of  $30 \text{ fb}^{-1}$  is required. Even though a combination of all channels as well as the data from both experiments are needed, new approaches and robust reconstruction algorithms will also be required.

Another primary goal of the  $D\bar{O}$  upgrade physics program is the study of the top quark. With an increase in the CM energy from 1.8 TeV to  $\approx 2$  TeV, the  $t\bar{t}$  production cross section will increase by about 38% (the production is dominated by  $q\bar{q} \rightarrow t\bar{t}$ .) For single top production the increase will be about 22% for the  $s$ -channel ( $q\bar{q} \rightarrow t\bar{b}$ ) and about 44% for the  $W$ -gluon fusion process ( $qg \rightarrow qt\bar{b}$ ). The expected uncertainty in the top quark mass measurement is  $\delta m_t \simeq 3$  GeV. The  $t\bar{t}$  production cross section is expected to be measured with about 9% accuracy. Production and decay properties will be studied in detail. For example,  $t\bar{t}$  spin correlations, which are transmitted to the decay products

since the top decays before hadronization, can be observed with an uncertainty on the spin correlation coefficient  $\kappa$  of  $\delta\kappa \simeq 0.4$ . Studies of the kinematic properties in  $t\bar{t}$  events will also be sensitive to physics beyond the standard model. For example, one can search for resonances in the invariant  $t\bar{t}$  mass spectrum, such as the  $Z'$  predicted by topcolor assisted technicolor [3].

In Run 2 we will also be able to observe single top production. Since this process involves production of a top quark at the  $Wtb$  vertex, it is sensitive to the magnitude of the CKM matrix element  $V_{tb}$ . A measurement of  $|V_{tb}|$  with accuracy better than  $\pm 15\%$  will be possible in Run 2. Furthermore, deviations from the  $V - A$  nature of the  $Wtb$  coupling can be probed.

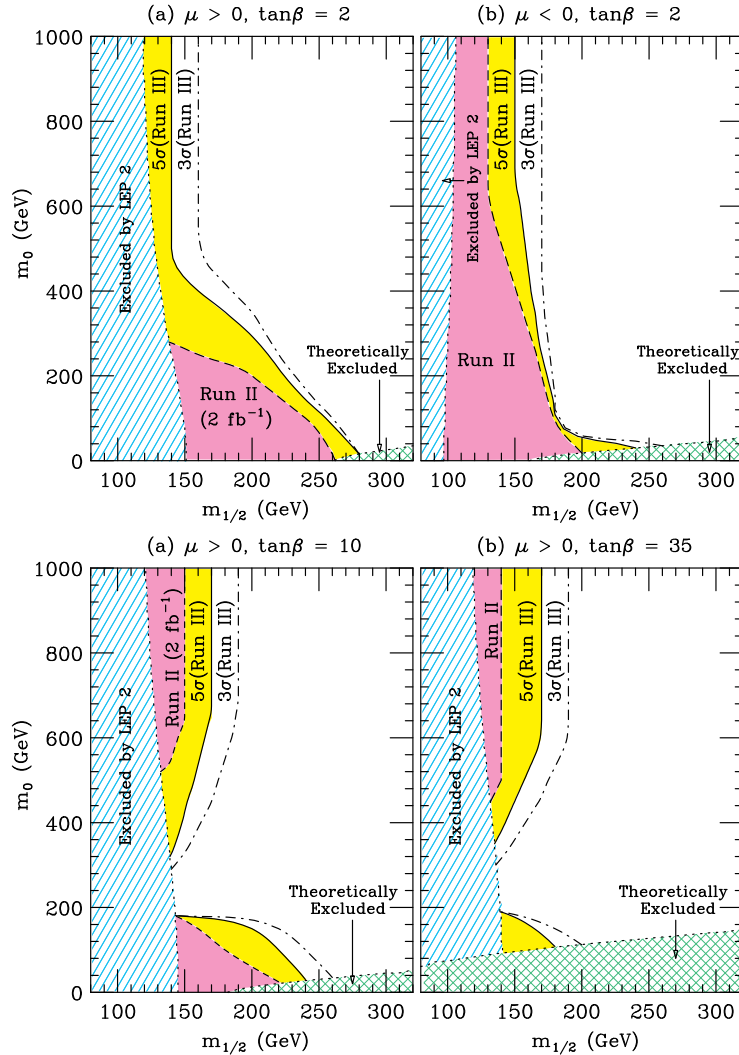


Figure 10: Contours of 99% C.L. observation in Run 2 ( $2 \text{ fb}^{-1}$ ) for gaugino pair production in the trilepton decay modes plotted in the  $(m_{1/2}, m_0)$  plane: (a)  $\tan\beta = 2, \mu > 0$ ; (b)  $\tan\beta = 2, \mu < 0$ ; (c)  $\tan\beta = 10, \mu > 0$ ; (d)  $\tan\beta = 35, \mu > 0$ . Also shown are the contours for a  $3\sigma$  observation and  $5\sigma$  discovery in Run 3 ( $30 \text{ fb}^{-1}$ ). From Ref. [8].

An important goal of electroweak physics in Run 2 is the measurement of the  $W$  boson

mass. With an integrated luminosity of  $2 \text{ fb}^{-1}$  per experiment the level of statistical precision will be of order 10 MeV and systematic errors in the measurement and model will dominate. An uncertainty of approximately  $\delta m_W = 30 \text{ MeV}$  from the combination of CDF and DØ measurements seems achievable [9].

The search for new phenomena will be another important part of the physics program in Run 2. Fig. 10 shows the potential for observing gaugino pair production in the trilepton decay modes  $p\bar{p} \rightarrow \tilde{\chi}_1^\pm \tilde{\chi}_1^\mp, \tilde{\chi}_1^\pm \tilde{\chi}_2^0 \rightarrow 3\ell + X$  plotted for the minimal supergravity framework in the  $(m_{1/2}, m_0)$  plane, where  $m_{1/2}$  and  $m_0$  are the universal scalar and fermion masses at the GUT scale. This process can probe  $m_{1/2}$  up to  $\sim 250 \text{ GeV}$  for favorable values of the model parameters, which corresponds to a gluino mass of  $\sim 600 \text{ GeV}$ . For large  $\tan\beta$ , stau decays of the gauginos will be dominant, resulting in tau lepton signatures. The upgraded DØ tracking system will improve the tau identification capabilities, thus aiding in this search.

Supersymmetric squark/gluino production in the jets+ $\cancel{E}_T$  channel is expected to probe masses up to about 350-375 GeV for  $2 \text{ fb}^{-1}$ . The sensitivity to stop and sbottom squarks depends on their decay modes: if  $\tilde{t} \rightarrow b\tilde{\chi}_1^\pm$  or  $\tilde{t} \rightarrow b\ell\tilde{\nu}$ , masses up to 250 GeV can be probed.

Interesting possibilities for utilizing the new capabilities of the upgraded detector exist in several scenarios of SUSY. For example, in gauge-mediated SUSY breaking the gravitino  $\tilde{G}$  is the LSP. If the  $\tilde{\chi}_1^0$  is the NLSP, then  $\tilde{\chi}_1^0 \rightarrow \gamma\tilde{G}$  and one can search for gaugino pair production using the  $\gamma\gamma + \cancel{E}_T$  final state. The excellent  $\cancel{E}_T$  resolution in DØ can be used and, if the decay has a long lifetime so that the photons are displaced from the primary vertex, the calorimeter and preshower detector can be used to project the photon back to the beamline with an uncertainty of  $\simeq 2 \text{ cm}$ . Alternatively, if the  $\tilde{\tau}$  is the NLSP then  $\tilde{\tau} \rightarrow \tau\tilde{G}$ , and the signature is  $\tau$ 's +  $\cancel{E}_T$ . If the  $\tilde{\tau}$  is long-lived, large impact parameter  $\tau$ 's or heavily ionizing  $\tilde{\tau}$ 's may then be important, which can be identified from large impact parameter tracks or high  $dE/dx$  in the SMT.

For an integrated luminosity of  $2 \text{ fb}^{-1}$  at the Tevatron approximately  $10^{11}$   $b$ -quark pairs will be produced. Therefore, a wide range of  $b$ -physics studies will be possible. These include  $b$ -quark cross sections, rare  $B$  decays,  $B_s$  mixing and CP violation in the  $B - \bar{B}^0$  system. In contrast to high  $p_T$  physics,  $B$  mesons are produced at relatively high  $\eta$  and low  $p_T$ . Therefore, tracking and vertexing out to  $\eta \approx 3$  is important for  $b$ -physics studies. Simulations indicate that  $B_s$  mixing could be detected for values of the mixing parameter  $x_s$  up to 30 for DØ and 60 for CDF, and that CP violation could be accessible with an error on  $\sin(2\beta)$  of about 0.04 for each experiment with  $2 \text{ fb}^{-1}$  of data. For more details see Ref. [10].

## Acknowledgments

I would like to thank the QFTHEP2001 organizers for arranging a stimulating conference and for their warm hospitality. My colleague Natasha Sotnikova deserves a special thanks for making my visit to Moscow one of the most memorable ones. I am also very thankful to Boaz Klima for reading this paper.

## References

- [1] J. Womersley, “Operation and Physics Potential of Tevatron Run 2, Fermilab-Conf-01-367-E.
- [2] T. Zimmerman, et al., IEEE Trans. Nucl. Sci. **42** (1995) 803.
- [3] Report on “The DØ upgrade: The Detector and its Physics, Fermilab Pub-96/357-E; J. Ellison, “The DØ Detector Upgrade and Physics Program, hep-ex/0101048; N. Parashar, “The DØ Run II Detector and Physics Prospects, hep-ex/0105026”.
- [4] M.D. Petroff and M.G. Staplebroek, IEEE Trans. Nucl. Sci., **36**, No. 1 (1989) 158; M.D. Petroff and M. Attac, IEEE Trans. Nucl. Sci., **36**, No. 1 (1989) 163.
- [5] P. Baringer et al., (DØ Collaboration), “Cosmic Ray Tests of the DØ Preshower Detector”, submitted to Nucl. Instrum. Meth. A. hep-ex/0007026.
- [6] The LEP Higgs Working group, “Standard Model Higgs Boson at LEP: Results with the 2000 Data, Request for Running in 2001”.  
[http://lephiggs.web.cern.ch/LEPHIGGS/papers/doc\\_nov3\\_2000.ps](http://lephiggs.web.cern.ch/LEPHIGGS/papers/doc_nov3_2000.ps)
- [7] M. Carena et al., Report of the Tevatron Higgs Working Group, hep-ph/0010338.
- [8] S. Abel et al., Report of the SUGRA Working Group for Run II of the Tevatron, hep-ph/0003154.
- [9] R. Brock et al., Report of the Working Group on Precision Measurements, hep-ex/0011009.
- [10] V. Kuznetsov, “Higgs and  $B$  physics in Run II”, QFT2000 proceedings.